DOI: 10.1002/ejic.200900839

Solvothermal Synthesis and Characterization of Hierarchically Nanostructured Hydroxyapatite Hollow Spheres

Ming-Guo Ma*[a] and Jie-Fang Zhu[b]

Keywords: Materials science / Nanostructures / Self-assembly

Hierarchically nanostructured hydroxyapatite (HA) hollow spheres assembled from nanorods have been successfully synthesized using $CaCl_2$, NaH_2PO_4, and potassium sodium tartrate via a solvothermal method at 200 °C for 24 h in water/*N*,*N*-dimethylformamide (DMF) mixed solvents. The ratio of water to DMF plays a key role in the formation of hierarchically nanostructured HA hollow spheres. The potassium sodium tartrate was used as a chelating ligand and a template molecule in the synthesis and self-assembly of HA nanorods. The products were characterized by X-ray powder diffraction, and field-emission scanning electron microscopy (FESEM), transmission electron microscopy, high-resolution transmission electron microscopy (HRTEM), energy-dispersive X-ray spectra (EDS), Brunauer–Emmett–Teller (BET), and Fourier transform infrared spectrometry. FESEM and TEM images indicated that hollow spheres of about 3.6 μm in diameter were built by HA nanorods. On the basis of experimental results, a possible formation mechanism of these hierarchically nanostructured HA hollow spheres in the growth processes was proposed.

Introduction

Hierarchical nanostructured hollow spheres have attracted a great amount of attention because of their novel optical,[1] magnetic,[2] catalytic,[3–5] other related properties and potential applications in drug delivery,[6–8] gas sensors,[9,10] water treatment,[11] and hydrogen storage.[12] Up to now, a variety of hollow spheres such as TiO_2,[13] Cu_2O,[14] WO_3,[15] MnS,[16] and In_2S_3[17] have been reported. Various methods including coprecipitation, microemulsion,[18] ultrasound irradiation, hydrothermal method,[19] and thermal decomposition of organometallic compounds have been applied in producing the hollow sphere structures.

As an important bioactive material, hydroxyapatite [HA, $Ca_{10}(PO_4)_6(OH)_2$] has attracted a great amount of attention and it is used as a bone cement, drug deliverer, tooth paste additive, dental implant, gas sensor, ion exchange, catalyst, catalyst support, and host material for lasers, owing to its excellent osteoconductivity, biocompatibility, bioactivity, and chemical and biological similarity with the mineral constituents of human bones and teeth.[20–22] Up to date, some successful strategies including precipitation,[23] hydrothermal,[24] sol-gel,[25] emulsion, microemulsion,[26] and microwave irradiation[27] have been employed for the synthesis of HA. Recently, Wu et al.[28] fabricated HA nanoribbon spherulites using the bioactive eggshell membrane as a directing template in the presence of ethylenediamine in a one-step reaction. Li et al.[29] reported the fabrication of HA nanorods by tuning the interfaces between surfactants and the central atoms of HA based on the liquid-solid solution strategy. Imai et al.[30] synthesized needles, fibers, and sheets of HA through the hydrolysis of a solid precursor crystal of dicalcium phosphate in an alkali solution by varying the pH and ion concentrations. Huang et al.[31] reported the synthesis of flower-like porous B-type carbonated HA microspheres by the bubble-template route. We synthesized agglomerated nanorods of HA using monetite as a precursor in a NaOH solution and HA microtubes using $CaCl_2$ and NaH_2PO_4 in mixed solvents of water/DMF by a solvothermal method at 160 °C for 24 h.[32,33] However, to the best of our knowledge, there has been no report on the synthesis of hierarchically nanostructured HA hollow spheres assembled from nanorods until now. It is highly desirable to achieve a synthesis of hierarchically nanostructured HA hollow spheres because of their high surface areas and potential applications in high-capacity drug loading and targeted drug delivery as well as in other biomedical purposes.[34–36]

Herein, we report a simple, facile, and economical solvothermal approach to the fabrication of hierarchically nanostructured HA hollow spheres assembled from nanorods. The potassium sodium tartrate was used as a chelating ligand inducing the synthesis and self-assembly of the HA nanorods. The ratio of DMF to water had a significant in-

[a] College of Materials Science and Technology, Beijing Forestry University,
Beijing 100083, P. R. China
Fax: +86-10-62338149
E-mail: mg_ma@bjfu.edu.cn
[b] Department of Materials Chemistry, The Ångström Laboratory, Uppsala University,
Uppsala 75121, Sweden

fluence on the synthesis of HA hollow spheres. We also discuss the possible formation mechanism of these hollow spheres in brief. Of all the methods, the solvothermal process is a promising technology for preparation of nanomaterials due to its many advantages. It can not only evidently decrease the reaction temperature of systems, but also prepare highly crystalline products with narrow size distribution, high purity, and low aggregation. The morphology and crystal structure of the products can be controlled by adjusting the solvothermal reaction conditions. The potassium sodium tartrate can act as a template molecule to form nanomaterials with desired morphologies.[37,38]

Results and Discussion

Figure 1 (a) shows the XRD pattern of the typical sample, synthesized in mixed solvents of water (4 mL) and DMF (11 mL) by a solvothermal method at 200 °C for 24 h. All the peaks in the XRD pattern can be indexed to a pure phase of well-crystalline HA with a hexagonal structure (JCPDS 84-1998) and space group $P21/n$ (#14) with lattice constants (a = 6.800, b = 7.023, c = 6.471). No peaks from impurities such as $CaHPO_4$ and $Ca(OH)_2$ were observed, indicating the complete reaction of the $CaCl_2$ and NaH_2PO_4. To verify the functional groups of HA, the FTIR spectra was studied, as shown in part b of Figure 1. The broad strong peak at around 3428 cm^{-1} should belong to the absorbed water on HA.[39] It is well known that the characteristic stretching mode of the –OH vibration in HA is located at around 3570 cm^{-1},[40] which can be observed in Figure 1 (b), although the peak was very weak because of an overlap with the broad strong peak of the absorbed water on HA. The bending mode of the OH– vibration was observed at 1616 cm^{-1}. The intense peaks located at 1033, 601, and 567 cm^{-1} can be attributed to the PO_4^{3-}.[41] On the basis of the result, we can confirm that the sample obtained is HA.

The morphologies of the sample were investigated with FESEM. Figure 2 shows FESEM micrographs of the same sample as in Figure 1, from which one can see HA with a hierarchical hollow sphere nanostructure assembled from nanorods. Figure 2 (b) shows a typical broken sphere, confirming the hollow structure inside. From the side of the spheres, one can see that hundreds of nanorods assemble. Figure 2 (c) displays an individual hollow sphere with a diameter of ≈3.6 μm. From the detailed structure of the hollow sphere in Figure 2 (d), one can see the nanorods with relatively uniform size and size distribution. This is the first report on the fabrication of the hierarchically nanostructured HA hollow spheres assembled from nanorods.

The morphologies and microstructures of the samples were further investigated by TEM, HRTEM, and EDS. Figure 3 (a) shows a TEM micrograph of the HA, from which one can see hierarchically nanostructured HA hollow spheres with similar size. Figure 3 (b) shows an individual HA hollow sphere, and the nanorods arrange by self-assembly. From the detailed structure of the hollow sphere in

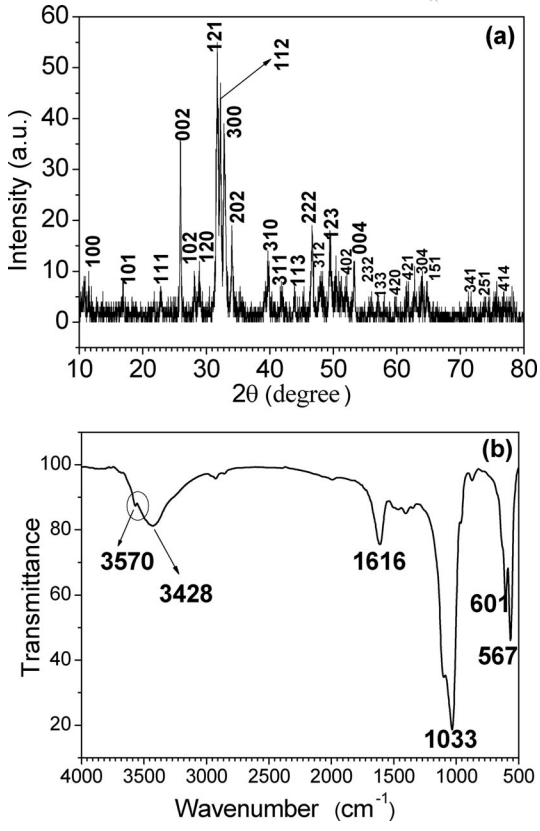

Figure 1. (a) A typical XRD pattern and (b) FTIR spectrum of HA powder prepared by a solvothermal method in mixed solvents of water (4 mL) and DMF (11 mL) at 200 °C for 24 h.

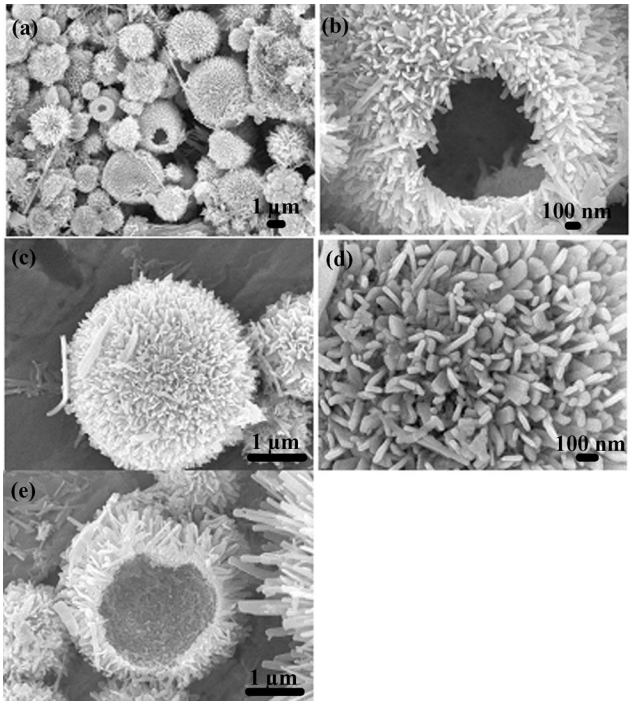

Figure 2. SEM micrographs of hierarchically nanostructured HA hollow spheres.

Figure 3 (c), the nanorods have relatively uniform size and size distribution. Figure 3 (d) shows the HRTEM micrograph of the HA nanorod, which indicates the single crystalline structure of the nanorod. The periodic fringe spacing of 3.43 Å corresponds to the d-spacing of (002) planes of the hexagonal HA. The composition of the typical product was further confirmed by using EDS analysis. The peaks of O, P, and Ca were obviously observed without any other impure peaks in the EDS spectrum (Figure 4), which confirm that the hollow sphere is pure HA.

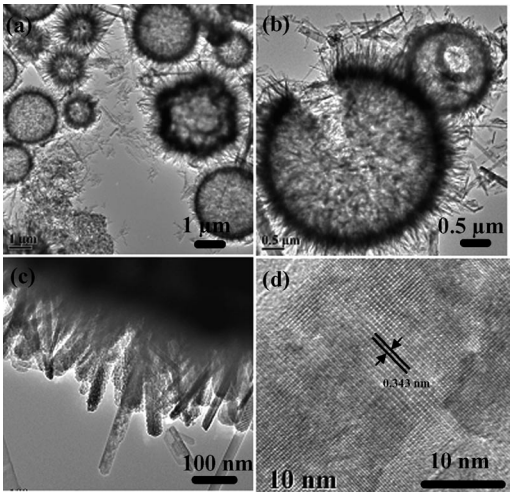

Figure 3. TEM micrographs of hierarchically nanostructured HA hollow spheres. (a) A typical TEM micrograph; (b) a HA hollow sphere; (c) a detailed structure of the hollow sphere; (d) the corresponding HRTEM image of an individual nanorod.

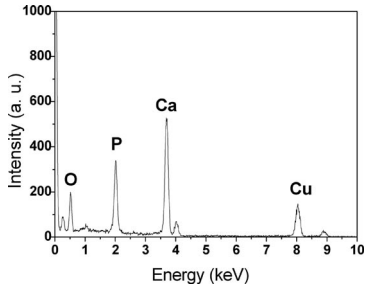

Figure 4. EDS spectrum of hierarchically nanostructured HA hollow spheres.

Figure 5 shows the N_2 adsorption/desorption isotherm and the corresponding pore size distribution of the prepared hierarchically nanostructured HA hollow spheres. The measurement shows that the BET surface area was 40.53 m^2/g. The BJH (Barett–Joyner–Halenda) desorption average pore size of these spheres was ca. 19.37 nm, and the single-point adsorption total volume at $P/P_0 = 0.969$ of HA was 0.153 cm^3/g.

To investigate the possible formation mechanism of hierarchically nanostructured HA hollow spheres, the HA samples were prepared at 200 °C for different heating times and different ratios of water to DMF, while other reaction conditions were kept the same. Figure 6 shows SEM micrographs of the samples prepared by solvothermal method at 200 °C for 3 h, 6 h, and 12 h, respectively. When the heating time was 3 h (Figure 6, a), many nanoparticles and nanorods were observed. When the heating time was increased to 6 h, the congeries and bundles of nanorods dominated (Figure 6, b). When the heating time was increased to 12 h, the nanorods were assembled to form the flower-like morphology (Figure 6, c). From Figure 6, one can clearly see that the number of congeries and the degree of assembly increased with time. The individual nanorods, bundled nanorods, and flower-like morphology also were observed in short synthesis cases. The ratio of water to DMF had a significant effect on the size and morphology of samples. When the ratio of water to DMF was 4:11, the hierarchically nanostructured HA hollow spheres were obtained (Figure 2 and Figure 3). However, when the ratio of water to DMF was 2:1, the flower-like morphologies assembled from nanosheets formed, and hierarchically nanostructured HA hollow spheres were not observed (Figure 7, a). The sizes and morphologies of flower-like HA were relatively uniform. When the ratio of water to DMF was 1:4, the hierarchically nanostructured HA hollow spheres were observed as a major product and the nanosheets were observed as a minor product (Figure 7, b). When the ratio of water to DMF was 2:13, the hollow spheres were obtained as a minor product, and many irregular morphology aggregations and big sheets appeared (Figure 7, c). When only

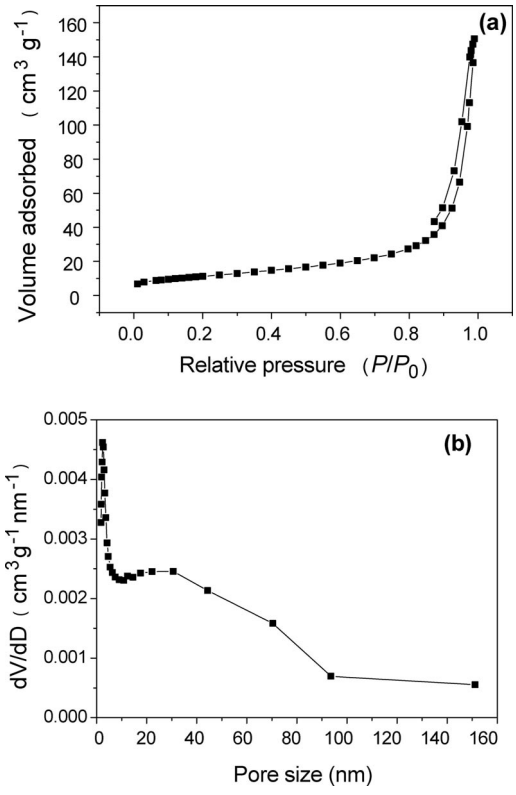

Figure 5. (a) N_2 adsorption/desorption isotherm of hierarchically nanostructured HA hollow spheres and (b) the corresponding pore size distribution.

DMF was used as the solvent, the nanoparticles and big sheets formed (Figure 7, d). Therefore, the appropriate ratio of water to DMF is important for the formation of hierarchically nanostructured HA hollow spheres.

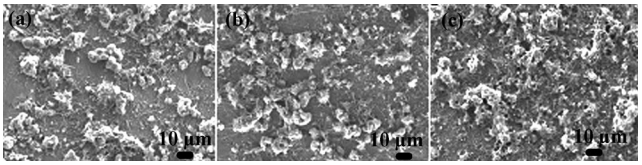

Figure 6. SEM micrographs of the samples prepared by solvothermal method at 200 °C for different times: (a) 3 h; (b) 6 h; and (c) 12 h.

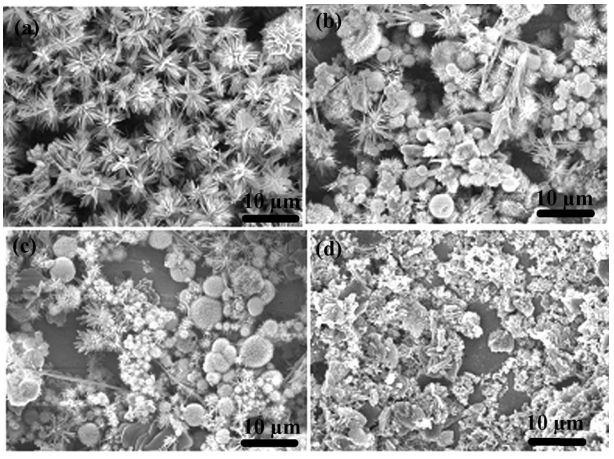

Figure 7. SEM micrographs of samples prepared by solvothermal method at different ratio of water to DMF at 200 °C for 24 h: (a) water (10 mL) and DMF (5 mL); (b) water (3 mL) and DMF (12 mL); (c) water (2 mL) and DMF (13 mL); (d) water (0 mL) and DMF (15 mL).

On the basis of experimental results, self-assembly base-erosion is suggested as a possible formation mechanism to form hierarchically nanostructured HA hollow spheres. This mechanism was also suggested for the formation of ZnO hollow spheres.[42] The base-erosion mechanism involves initial nucleation, growth, aggregation, and erosion. At the initial stage, the HA nanorods are first formed by nucleation and the nanorod-like morphology is shaped due to the anisotropy of HA. Then, the individual nanorods aggregate into a bundle-like morphology in a three-dimensional array. The number of congeries and the degree of assembly increased along with the increase of reaction time and thus the flower-like or sphere-like morphology assembled from nanorods was obtained. After that, the existence of a larger amount of base causes the flower-like or sphere-like morphology to erode from the center to the outside in succession due to the high calcium concentration in the center, which means the center of the spheres have the fastest erosion velocity. Finally, hierarchically nanostructured HA hollow spheres were obtained. Figure 8 illustrates the formation mechanism of hierarchically nanostructured HA hollow spheres assembled from nanorods. The individual nanorods, bundle-like nanorods, and flower-like morphology can be observed from Figure 6. The potassium sodium tartrate was used as a chelating ligand inducing the synthesis and self-assembly of HA nanorods. In the presence of $C_4H_4O_6^{2-}$, the complex of Ca^{2+}-tartrate formed due to the strong coordination ability of $C_4H_4O_6^{2-}$.[43] The $C_4H_4O_6^{2-}$ was also used for the formation of CuO spheres[37] and Cu_2O nanocages.[38] When the potassium sodium tartrate was not present, the HA hollow spheres were not observed and HA microtubes formed.[33] In the experiment, when we reduced the amount of DMF to some extent, the HA hollow spheres were not obtained and the flower-like morphology assembled from nanosheets was formed (Figure 7, a). The number of HA hollow spheres formed increased with increasing concentration of DMF (Figures 2 and 3). The phase and morphology of product strongly depended on the properties of the solvent and the pH value of the reaction mixture.[44] It is well known that DMF is a weakly basic additive. When heated, the DMF began to release NH_3^+ and thus provided a basic condition for the nucleation and growth of HA. Low concentration of DMF and inadequate heating time could not provide enough of the basic condition. However, when the concentration of DMF was too high, the HA hollow spheres were also not obtained because of too rapid nucleation and growth of HA (Figure 7, d), which has been reported previously.[33] So an appropriate amount of DMF is a key factor in forming HA hollow spheres. We have also revealed the effect of the ratio of DMF/water in mixed solvents on the solvothermal HA microtube synthesis and clearly observed the evolution process of the phase and morphology of the product along with increasing heating time.[33] Although a self-assembly base-erosion mechanism was proposed in consideration of current experimental results, the intrinsic and detailed formation mechanism of hierarchically nanostructured HA hollow spheres needs to be further explored.

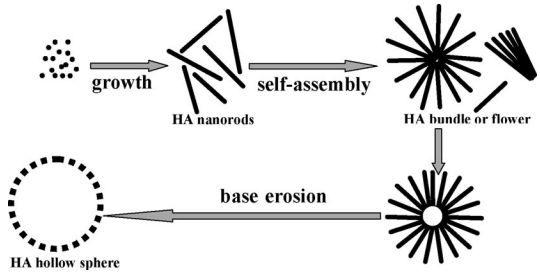

Figure 8. Schematic representation of the formation mechanism of hierarchically nanostructured HA hollow spheres.

Conclusion

In summary, we firstly report a novel, simple, and reliable solvothermal route to the synthesis of hierarchically nanostructured HA hollow spheres. The ratio of water to DMF determines the formation of the hollow nanostructures. A rational mechanism of self-assembly base-erosion to form

the hierarchically nanostructured HA hollow spheres is also proposed. This synthesis' strategy perhaps opens a new window to the preparation of hollow nanostructures.

Experimental Section

General: All chemicals were of analytical grade and used as received without further purification. All experiments were conducted under air. A typical synthesis experiment occurred as follows: $CaCl_2$ (0.110 g), $C_4H_4O_6KNa{\cdot}4H_2O$ (0.282 g) (potassium sodium tartrate), and NaH_2PO_4 (0.094 g) were added into mixed solvents of DMF (11 mL) and deionized water (4 mL) under vigorous stirring for 30 min. The solution was transferred into a 20-mL Teflon-lined stainless steel autoclave. The autoclave was maintained at 200 °C for 24 h. The product was separated from the solution by centrifugation, washed with water and ethanol several times and dried at 60 °C. Finally, a white powder was obtained. By adjusting the reaction condition, we can obtain high morphological yield of HA hollow spheres.

XRD patterns were recorded at a scanning rate of 0.12 s^{-1} in the 2θ range 10–70° on a D/MAX 2200 (Rigaku, Japan) diffractometer operating at 40 kV with Cu-K_α (λ = 1.5405 Å) radiation. FESEM micrographs were recorded with a JSM-6700F field-emission scanning electron microscope. All samples were Au-coated prior to examination by FESEM. TEM imaging, HRTEM imaging, and EDS were performed with a JEOL JEM-2010 electron microscope with an accelerating voltage of 200 kV. FTIR spectroscopy was carried out with a Thermo Nicolet Nexus spectrometer, using the KBr disk method. The BET surface area and pore size distribution were measured with an accelerated surface area and porosimetry system (ASAP 2010).

Acknowledgments

Financial support from the Beijing Forestry University Young Scientist Fund (BLX2W8010), China Postdoctoral Science Foundation, Ångpanneföreningen's Foundation for Research and Development (ref. nr 09-370), Major State Basic Research Development Program of China (973 Program) (No. 2010CB732204), and China Ministry of Education (No. 111) is gratefully acknowledged.

[1] G. T. Duan, W. P. Cai, Y. Y. Luo, F. Q. Sun, *Adv. Funct. Mater.* **2007**, *17*, 644–650.
[2] G. T. Duan, W. P. Cai, Y. Y. Luo, Z. G. Li, Y. Lei, *J. Phys. Chem. B* **2006**, *110*, 15729–15733.
[3] D. Chen, J. H. Ye, *Adv. Funct. Mater.* **2008**, *18*, 1922–1928.
[4] X. F. Song, L. Gao, *J. Phys. Chem. C* **2008**, *112*, 15299–15305.
[5] S. J. Guo, S. J. Dong, E. K. Wang, *J. Phys. Chem. C* **2009**, *113*, 5485–5492.
[6] W. Wei, G. H. Ma, G. Hu, D. Yu, T. Mcleish, Z. G. Su, Z. Y. Shen, *J. Am. Chem. Soc.* **2008**, *130*, 15808–15810.
[7] H. Zhao, J. F. Chen, Y. Zhao, L. Jiang, J. W. Sun, J. Yun, *Adv. Mater.* **2008**, *20*, 3682–3686.
[8] S. W. Cao, Y. J. Zhu, *J. Phys. Chem. C* **2008**, *112*, 12149–12156.
[9] H. G. Zhang, Q. S. Zhu, Y. Zhang, Y. Wang, L. Zhao, B. Yu, *Adv. Funct. Mater.* **2007**, *17*, 2766–2771.
[10] J. H. Lee, *Sens. Actuat. B: Chem.* **2009**, *140*, 319–336.
[11] J. B. Fei, Y. Cui, X. H. Yan, W. Qi, Y. Yang, K. W. Wang, Q. He, J. B. Li, *Adv. Mater.* **2008**, *20*, 452–456.
[12] B. Z. Fang, M. Kim, J. H. Kim, J. S. Yu, *Langmuir* **2008**, *24*, 12068–12072.
[13] X. X. Li, Y. J. Xiong, Z. Q. Li, Y. Xie, *Inorg. Chem.* **2006**, *45*, 3493–3495.
[14] H. G. Zhang, Q. S. Zhu, Y. Zhang, Y. Wang, L. Zhao, B. Yu, *Adv. Funct. Mater.* **2007**, *17*, 2766–2771.
[15] D. Chen, J. H. Ye, *Adv. Funct. Mater.* **2008**, *18*, 1922–1928.
[16] Y. Cheng, Y. S. Wang, C. Jia, F. Bao, *J. Phys. Chem. B* **2006**, *110*, 24399–24402.
[17] S. F. Shao, G. J. Zhang, H. J. Zhou, N. J. Guan, T. H. Chen, *Acta Physico-Chimica Sinica* **2009**, *25*, 411–416.
[18] D. H. M. Buchold, C. Feldmann, *Nano Lett.* **2007**, *7*, 3489–3492.
[19] L. Fan, R. Guo, *J. Phys. Chem. C* **2008**, *112*, 10700–10706.
[20] D. A. Wahl, J. T. Czernuszka, *Eur. Cells Mater.* **2006**, *11*, 43–56.
[21] A. L. Boskey, M. F. Young, T. Kilts, K. Verdelis, *Cells Tissues Organs* **2005**, *181*, 144–153.
[22] S. V. Dorozhkin, *J. Mater. Sci.* **2007**, *42*, 1061–1095.
[23] S. Kannan, A. F. Lemos, J. M. F. Ferreira, *Chem. Mater.* **2006**, *18*, 2181–2186.
[24] A. A. Chaudhry, S. Haque, S. Kellici, P. Boldrin, I. Rehman, F. A. Khalid, J. A. Darr, *Chem. Commun.* **2006**, *21*, 2286–2288.
[25] A. Bigi, E. Boanini, K. Rubini, *J. Solid State Chem.* **2004**, *177*, 3092–3098.
[26] G. K. Lim, J. Wang, S. C. Ng, C. H. Chew, L. M. Gan, *Biomaterials* **1997**, *18*, 1433–1439.
[27] A. López-Macipe, J. Gómez-Morales, R. Rodríguez-Clemente, *Adv. Mater.* **1998**, *10*, 49–53.
[28] J. K. Liu, Q. S. Wu, Y. P. Ding, *Eur. J. Inorg. Chem.* **2005**, 4145–4149.
[29] X. Wang, J. Zhuang, Q. Peng, Y. D. Li, *Adv. Mater.* **2006**, *18*, 2031–2034.
[30] H. Ito, Y. Oaki, H. Imai, *Cryst. Growth Des.* **2008**, *8*, 1055–1059.
[31] X. K. Cheng, Q. J. He, J. Q. Li, Z. L. Huang, R. A. Chi, *Cryst. Growth Des.* **2009**, *9*, 2770–2775.
[32] M. G. Ma, Y. J. Zhu, J. Chang, *J. Phys. Chem. B* **2006**, *110*, 14226–14230.
[33] M. G. Ma, Y. J. Zhu, J. Chang, *Mater. Lett.* **2008**, *62*, 1642–1645.
[34] Y. J. Wang, X. D. Wang, K. Wei, N. R. Zhao, S. H. Zhang, J. D. Chen, *Mater. Lett.* **2007**, *61*, 1071–1076.
[35] M. Y. Ma, Y. J. Zhu, L. Li, S. W. Cao, *J. Mater. Chem.* **2008**, *18*, 2722–2727.
[36] Y. S. Wang, M. S. Hassan, P. Gunawan, R. Lau, X. Wang, R. Xu, *J. Colloid Interface Sci.* **2009**, *339*, 69–77.
[37] Y. Y. Xu, D. R. Chen, X. L. Jiao, *J. Phys. Chem. B* **2005**, *109*, 13561–13566.
[38] C. H. Lu, L. M. Qi, J. H. Yang, X. Y. Wang, D. Y. Zhang, J. L. Xie, J. M. Ma, *Adv. Mater.* **2005**, *17*, 2562–2567.
[39] R. N. Panda, M. F. Hsieh, R. J. Chung, T. S. Chin, *J. Phys. Chem. Solids* **2003**, *64*, 193–199.
[40] V. Jokanović, D. Izvonar, M. Dramićanin, B. Jokanović, V. Živojinović, D. Marković, B. Dačić, *J. Mater. Sci. Mater. Med.* **2006**, *17*, 539–546.
[41] T. A. Kriakose, S. K. Narayana, M. Palanichamy, D. Arivuoli, K. Dierks, G. Bocelli, C. Betzel, *J. Cryst. Growth* **2004**, *263*, 517–523.
[42] Z. T. Chen, L. Gao, *Cryst. Growth Des.* **2008**, *8*, 460–464.
[43] E. V. Shlyakhova, N. F. Yudanov, Yu. V. Shubin, L. I. Yudanova, L. G. Bulusheva, A. V. Okotrub, *Carbon* **2009**, *47*, 1701–1707.
[44] L. C. Chow, *J. Ceram. Soc. Jpn.* **1991**, *99*, 954–964.

Received: August 25, 2009
Published Online: November 4, 2009

